Simultaneous Acquisition of Polarimetric SVBRDF and Normals

Supplemental Material

SEUNG-HWAN BAEK and DANIEL S. JEON, KAIST
XIN TONG, Microsoft Research Asia
MIN H. KIM, KAIST

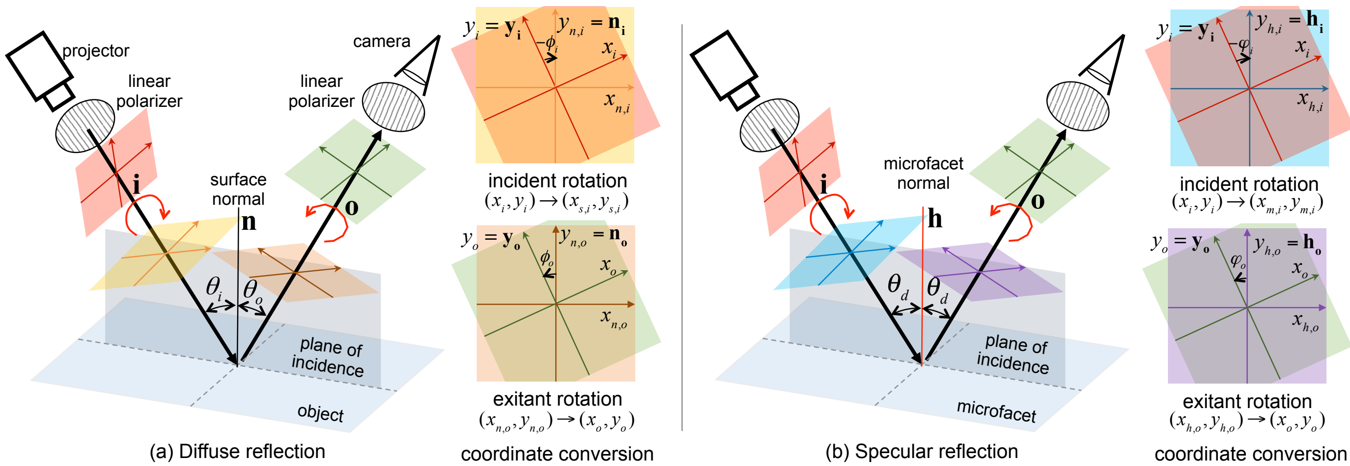

Fig. 1. Polarimetric diffuse vs. specular light transport. Two linear polarization filters are installed in front of a unpolarized projector and a camera. (a) The diffuse component of the polarized light is reflected on the object surface. The coordinate basis of the incident light stoke vector is converted to the incident coordinate system and then transformed to that of the camera. (b) According to the microfacet theory, the specular component is reflected on the facet surface, of which normal is same as the halfway vector. The coordinate basis of the incident stoke vector is converted w.r.t. the incident coordinate system, where the microfacet normal stands. (Insets) The incident/exitant rotation angles show rotation transformations about the z-axis, which is the direction of the light propagating.

ACM Reference Format:
Seung-Hwan Baek, Daniel S. Jeon, Xin Tong, and Min H. Kim. 2018. Simultaneous Acquisition of Polarimetric SVBRDF and Normals: Supplemental Material. *ACM Trans. Graph.* 37, 6, Article 268 (November 2018), 4 pages. https://doi.org/10.1145/3272127.3275017

1 FOUNDATIONS OF POLARIZATION

1.1 Mueller Transformation

Converting Coordinate Systems. A stoke vector of a light ray is defined with respect to a vector coordinate system, where the z-axis is aligned along the propagation direction of the light, the orientations of the x and y axes vary depending on the polarization state of the light. Before applying any transformation on a stoke vector, the coordinate system of the stoke vector should be adjusted to the same system of the transformation. Figure 1 depicts examples of the conversion of polarization coordinate systems.

We employ a coordinate rotation Mueller matrix for converting coordinate systems before applying a Mueller matrix to the stoke vector of the polarized light [Collett 2005]. A coordinate rotation Mueller matrix $\mathbf{C}$ rotates a stoke vector by the counter-clockwise angle ϑ about the z-axis, of which direction indicates the propagating direction of the light. The rotation matrix is mainly used for transforming a stoke vector coordinate system to that of a Mueller transformation matrix that we are applying:

$$\mathbf{C}(\vartheta) = \begin{bmatrix} 1 & 0 & 0 & 0 \\ 0 & \cos 2\vartheta & \sin 2\vartheta & 0 \\ 0 & -\sin 2\vartheta & \cos 2\vartheta & 0 \\ 0 & 0 & 0 & 1 \end{bmatrix}. \tag{1}$$

In case of diffuse polarization, $\mathbf{C}_{\mathrm{i}\rightarrow\mathrm{n}}(-\phi_i)$ is the conversion matrix from the coordinate system of the polarized light to the system of the incident polarization that is the incident coordinate system

Part of this work was done during Seung-Hwan Baek's internship at Microsoft Research Asia.
Authors' addresses: Seung-Hwan Baek; Daniel S. Jeon, KAIST, School of Computing, Daejeon, South Korea, 34141; Xin Tong, Microsoft Research Asia, Beijing, China, 100080; Min H. Kim, KAIST, School of Computing, Daejeon, South Korea, 34141, minhkim@kaist.ac.kr(corresponding-author).

0730-0301/2018/11-ART268 $15.00
https://doi.org/10.1145/3272127.3275017

(with the plane of incidence that holds normal $\mathbf{n}$), where the Fresnel/unpolarized Mueller matrices are defined. $\mathbf{C}_{\mathrm{n}\to\mathrm{o}}(\phi_o)$ is the conversion matrix from the exitant polarization system to the camera polarization system. Before applying the Mueller matrices, the coordinate system should be transformed from the y_i axis of the coordinate system of the incident light stoke vector to the $y_{n,i}$ axis of the incoming surface coordinate system (by rotating it with an angle of $-\phi_i$ about the z-axis) and then transformed from the $y_{n,o}$ axis of the outgoing surface stoke vector to the y_o axis of the camera coordinate system (by rotating it with ϕ_o).

In case of specular polarization, where $\mathbf{C}_{\mathrm{i}\to\mathrm{h}}(-\varphi_i)$ is the coordinate conversion matrix from the light ray (x_i, y_i) to the plane of incidence (that holds the halfway vector $\mathbf{h}$ of the microfacet normal) $(x_{h,i}, y_{h,i})$, where the Fresnel Mueller reflection matrix is defined, and $\mathbf{C}_{\mathrm{h}\to\mathrm{o}}(\varphi_o)$ is the conversion matrix from the facet normal $(x_{h,i}, y_{h,i})$ to the camera (x_o, y_o).

Fresnel Matrices. A Fresnel matrix can be used for formulating either transmission or reflection of the polarized light in a form of a Mueller matrix $\mathbf{F}^{\mathrm{F}\in\{\mathrm{T},\mathrm{R}\}}$:

$$\mathbf{F}^{\mathrm{F}\in\{\mathrm{T},\mathrm{R}\}} = \begin{bmatrix} \frac{F^\perp+F^\parallel}{2} & \frac{F^\perp-F^\parallel}{2} & 0 & 0 \\ \frac{F^\perp-F^\parallel}{2} & \frac{F^\perp+F^\parallel}{2} & 0 & 0 \\ 0 & 0 & \sqrt{F^\perp F^\parallel}\cos\delta & \sqrt{F^\perp F^\parallel}\sin\delta \\ 0 & 0 & -\sqrt{F^\perp F^\parallel}\sin\delta & \sqrt{F^\perp F^\parallel}\cos\delta \end{bmatrix}, \quad (2)$$

where F can be either Fresnel transmission coefficients T or reflection coefficients R, and the δ is the retardation phase shift between the perpendicular and parallel waves, either π or 0. For a dielectric surface, $\cos\delta = -1$ when the incident angle is less than the Brewster angle; $\cos\delta = 1$, otherwise, and vice versa for $\sin\delta$. Here $T^\perp$ and $T^\parallel$ are the Fresnel transmission coefficients for the perpendicular (denoted by $\perp$) and the parallel ($\parallel$) components, respectively. When calculating $T^\perp$ and $T^\parallel$, θ_1 and θ_2 are the incident and exitant angles, and η_1 and η_2 are the refractive indices of the medium before and after the interface, respectively.

In our diffuse reflectance model, when we calculate incident Fresnel transmission coefficients, η_1 and η_2 are set to 1.0 and the object refractive index η, respectively. $\cos\theta_1$ and $\cos\theta_2$ are defined as $\cos\theta_1 = \mathbf{n}\cdot\mathbf{i}$ and $\cos\theta_2 = \sqrt{1-((1/\eta)\sin\theta_i)^2}$, respectively. In case of exitant transmission coefficients, η_1 and η_2 are switched as the object refractive index η and 1.0, respectively. $\cos\theta_1$ and $\cos\theta_2$ are defined as $\cos\theta_1 = \sqrt{1-((1/\eta)\sin\theta_2)^2}$ and $\cos\theta_2 = \mathbf{n}\cdot\mathbf{o}$, respectively following Snell's law. In addition, as a consequence of the conservation of energy, both $R^{\perp,\parallel}$ and $T^{\perp,\parallel}$ satisfy: $T^\perp + R^\perp = 1$ and $T^\parallel + R^\parallel = 1$.

Depolarization Matrix. The light absorbed by the object surface is completely unpolarized due to subsurface scattering with the object pigments. The diffuse absorption is formulated as a 4-by-4 depolarization scattering Mueller matrix $\mathbf{D}$, where the top-left element is the diffuse albedo ρ, and the rest of elements are zero.

$$\mathbf{D} = \begin{bmatrix} \rho & 0 & 0 & 0 \\ 0 & 0 & 0 & 0 \\ 0 & 0 & 0 & 0 \\ 0 & 0 & 0 & 0 \end{bmatrix}, \quad (3)$$

where ρ corresponds to the diffuse albedo. We also adopt the depolarization matrix $\mathbf{D}$ in our diffuse reflection model.

Linear Polarizer Matrix. A Mueller transmission matrix $\mathbf{L}$ with a linear polarization angle ϑ is formulated as:

$$\mathbf{L}(\vartheta) = \frac{1}{2}\begin{bmatrix} 1 & \cos 2\vartheta & \sin 2\vartheta & 0 \\ \cos 2\vartheta & \cos^2 2\vartheta & \cos 2\vartheta \sin 2\vartheta & 0 \\ \sin 2\vartheta & \cos 2\vartheta \sin 2\vartheta & \sin^2 2\vartheta & 0 \\ 0 & 0 & 0 & 0 \end{bmatrix}. \quad (4)$$

2 FACET DISTRIBUTION & GEOMETRIC ATTENUATION

GGX distribution function D [Walter et al. 2007] is as follows:

$$D(\theta_h;\sigma) = \frac{\sigma^2}{\pi\cos^4\theta_h\left(\sigma^2+\tan^2\theta_h\right)^2}, \quad (5)$$

where σ is the roughness parameter.

Smith G function [Heitz 2014] accounts for the masking-shadowing effect as follows:

$$G(\theta_i,\theta_o;\sigma) = \left(\frac{2}{1+\sqrt{1+\sigma^2\tan^2\theta_i}}\right)\left(\frac{2}{1+\sqrt{1+\sigma^2\tan^2\theta_o}}\right). \quad (6)$$

Since the geometric terms, both D and G, determine how many microfacets are observed from the given view direction, these geometric terms are therefore independent of polarization.

3 POLARIMETRIC DECOMPOSITION

In advance to estimate both appearance and normals, we generate the polarimetric shading matrix $\mathbf{H}$ from at least nine polarimetric images with different angle of the linear filters. To this end, we solve an overdetermined system:

$$\underset{\mathbf{H}}{\text{minimize}}\ \|\mathbf{I} - \mathbf{\Phi}_{\mathrm{o}}^{\intercal}\mathbf{H}\mathbf{\Phi}_{\mathrm{i}}\|_2^2. \quad (7)$$

While Equation (7) is a per-pixel optimization, we can solve it efficiently by reformulating Equation (7).

Tensor Reformulation for Decomposition. We denote $\bar{\mathbf{H}} \in \mathbb{R}^{N\times4\times4}$ as a tensor consisting of polarimetric shading matrices $\mathbf{H}$ for every pixel, where N is the number of pixels. Captured intensities of every pixel is described as $\bar{\mathbf{I}} \in \mathbb{R}^{N\times n\times m}$. First, we repack the tensor $\bar{\mathbf{I}}$ as a matrix, of which dimension is $\bar{\mathbf{I}} \in \mathbb{R}^{n\times Nm}$. Intermediate matrix $\bar{\mathbf{H}}' \in \mathbb{R}^{4\times Nm}$ is then estimated by solving the standard least-square optimization: $\text{minimize}_{\bar{\mathbf{H}}'}\ \|\bar{\mathbf{I}} - \mathbf{\Phi}_{\mathrm{o}}^{\intercal}\bar{\mathbf{H}}'\|_2^2$. Second, we repack the estimated $\bar{\mathbf{H}}'$ as the dimension of $\mathbb{R}^{m\times4N}$ and solve another optimization problem: $\text{minimize}_{\bar{\mathbf{H}}}\ \|\bar{\mathbf{H}}' - \bar{\mathbf{H}}\mathbf{\Phi}_{\mathrm{i}}\|_2^2$, where $\bar{\mathbf{H}} \in \mathbb{R}^{4\times4N}$ is the polarimetric shading matrix for every pixel. Per-pixel polarimetric shading matrix $\mathbf{H}$ is finally obtained by repacking $\bar{\mathbf{H}}$ as the dimension of $\mathbb{R}^{N\times4\times4}$.

4 NORMAL ESTIMATION

Our normal estimation consists of two stages where each stage exploit diffuse polarization and specular reflection respectively. In this supplemental material, we describe optimization details of each stage. For intuition and definition of terms, refer to the main paper.

Diffuse Normals. Diffuse polarization provides surface azimuth and zenith information with ambiguity [Kadambi et al. 2015]. Since we can estimate refractive index by jointly analyzing both the diffuse and the specular reflection, we can resolve the zenith ambiguity which comes from the unknown refractive index of materials. In order to resolve the remaining ambiguity of azimuth angle, we solve the following optimization function:

$$\begin{aligned}\underset{\mathbf{N}}{\text{minimize}}\ \ &\alpha_d \left\{\|\mathbf{W}\left(\mathbf{ON}-\mathbf{C}_z\right)\|_2^2+\|\mathbf{WAN}\|_2^2\right\}\\&+\beta_d\,\|\mathbf{GN}-\mathbf{N}_\mathrm{b}\|_2^2\ +\gamma_d\,\|\nabla\mathbf{N}\|_2^2\,,\end{aligned}\tag{8}$$

We then compute the derivative of the objective function with respect to $\mathbf{N}$ and set it as zero to obtain the following equation:

$$\begin{aligned}&\left(\alpha_d\mathbf{O}^\intercal\mathbf{W}^\intercal\mathbf{WO}+\alpha_d\mathbf{A}^\intercal\mathbf{W}^\intercal\mathbf{WA}+\beta_d\mathbf{G}^\intercal\mathbf{G}+\gamma_d\mathbf{K}^\intercal\mathbf{K}\right)\mathbf{N}\\&=\left(\alpha_d\mathbf{O}^\intercal\mathbf{W}^\intercal\mathbf{WC}_z+\beta_d\mathbf{G}^\intercal\mathbf{N}_\mathrm{b}\right),\end{aligned}\tag{9}$$

where $\mathbf{C}_z$ is the stacked matrix of $\cos(\theta_z)$ for every pixel and $\mathbf{K}$ is the matrix-form of the spatial gradient operator. We solve this equation in terms of $\mathbf{N}$ using gradient descent. Note that Equation (8) does not have unit-norm constraint for the surface normals. Since the constraint is non-linear with respect to the normals, we enforce it as a iterative approach solving Equation (8) and applying the unit-norm constraint iteratively. We empirically found that two iterations are sufficient to meet the constraint.

Specular Normals. In addition to having diffuse normal, we boost the surface normals for the region where zenith angle becomes close to zero by means of specular information. To this end, we solve the following optimization:

$$\begin{aligned}\underset{\mathbf{N}}{\text{minimize}}\ \ &\alpha_s\,\|\mathbf{W}\left(\mathbf{\Psi N}-\mathbf{C}_h\right)\|_2^2+\ \beta_s\,\|\mathbf{W}\nabla\mathbf{N}\|_2^2\\&+\gamma_s\,\|(1-\mathbf{W})\left(\mathbf{N}-\mathbf{N}'\right)\|_2^2\,,\end{aligned}\tag{10}$$

Computing the derivative with respect to $\mathbf{N}$ leads us to have the following equation:

$$\begin{aligned}&\left(\alpha_s\mathbf{\Psi}^\intercal\mathbf{W}^\intercal\mathbf{W\Psi}+\beta_s\mathbf{K}^\intercal\mathbf{W}^\intercal\mathbf{WK}+\gamma_s(1-\mathbf{W})^\intercal(1-\mathbf{W})\right)\mathbf{N}\\&=\left(\alpha_s\mathbf{\Psi}^\intercal\mathbf{W}^\intercal\mathbf{WC}_h+\gamma_s(1-\mathbf{W})^\intercal(1-\mathbf{W})\mathbf{N}'\right),\end{aligned}\tag{11}$$

where $\mathbf{C}_h$ is the stacked matrix of $\cos(\theta_h)$ for every pixel. Similar to diffuse normals, we also solve it using gradient descent and apply unit-norm constraint in a iterative manner.

Integrating Normals from RGB Channels. We can estimate normals from diffuse polarization for each color channel resulting in three different surface normals. Even though the estimated surface normals from different channels should be identical, we observe some difference between the surface normals due to SNR and wavelength-dependent scattering. We integrate the three normals from diffuse polarization through weighted averaging: $\mathbf{n}=\sum_{i=1}^{3}C_i\mathbf{n}_i$, where C_i is the weight of each color channel that penalizes the low SNR diffuse signal: $C_i=\mathbf{H}_{00}^{\mathrm{d}}/\sum_{i=1}^{3}\mathbf{H}_{00,i}^{\mathrm{d}}$. We used the averaged weight C_i per each material to be robust to noise.

5 ANALYSIS OF POLARIMETRIC REFLECTANCE MODEL

We here analyze each term of $\mathbf{H}$ shown in Figure 2 compared to our polarimetric model in details to further understand its characteristics. $\mathbf{H}_{00}$ shows both the diffuse and specular intensities which is well matched with our model: $\rho T_o^+T_i^++KR^+$. $\mathbf{H}_{11,22}$ mainly show

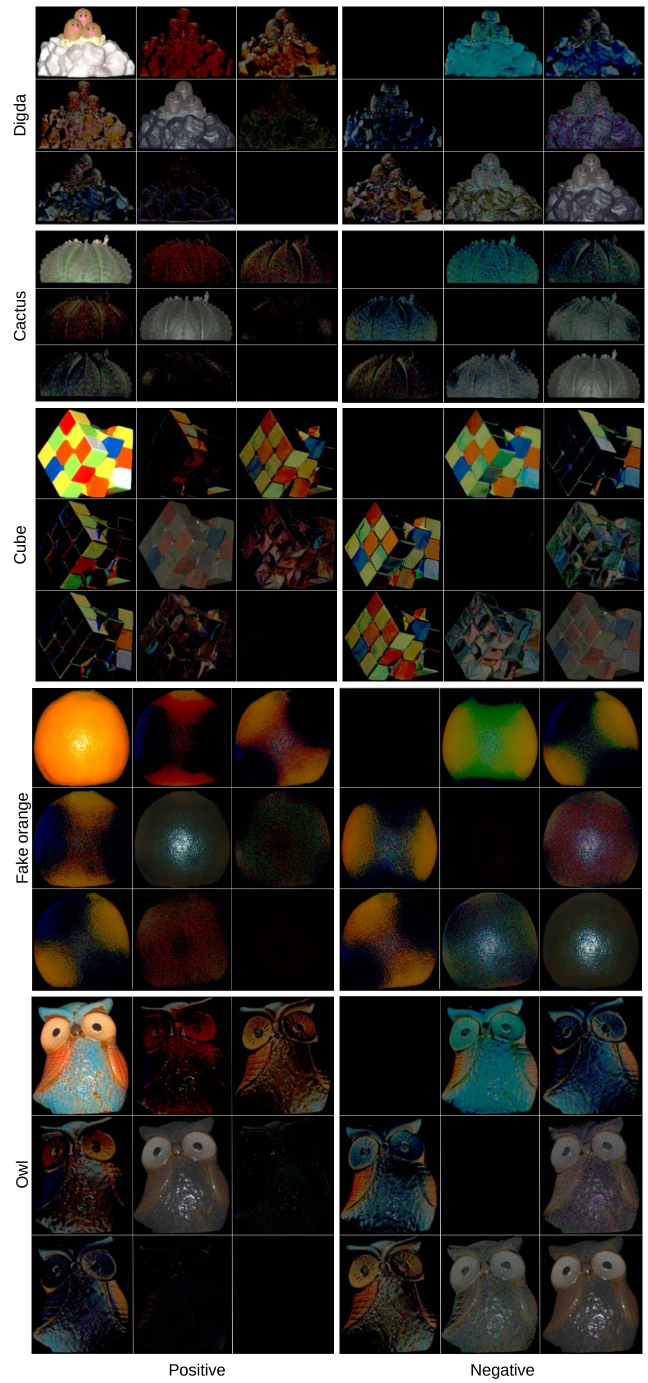

Fig. 2. Polarimetric shading matrix $\mathbf{H}$ of our real samples.

specular intensities and the two elements are similar to each other while the values are negative for (2,2). This observation is aligned with our model stating that the (1,1) and (2,2) elements can be modeled as KR^+ and $-KR^+$. $\mathbf{H}_{10,20}$ are related to the linear polarization state of the exitant light rays after the reflection as we termed exitant polarization. They exhibit low level of intensities compared to the diagonal components as expected in our modeling because of the Fresnel different term T_o^-. However, still we can see clear dependency on the surface azimuth. Our model explains this effect with β_o and α_o which are the cosine and sine values of the surface azimuthal angle. Also, we can observe that the intensity values become low for the surface where the zenithal angle becomes zero. This can be also explained by our model; T_o^- becomes close to zero when the surface zenith towards the camera. $\mathbf{H}_{01,02}$ correspond to the *incident polarization* describing how the polarization state of the incoming light affects the intensity of the captured image. Similar to the elements (1,0), (2,0), we can observe the dependency on the surface azimuth and zenith. However, these elements seem more sensitive to the color of the object pigments showing clear bluish color on the negative values. $\mathbf{H}_{12,21}$ deviate from our approximated model of the coaxial setup where they have visible negative intensities. However, note that our model under the real setup explains this phenomena well shown in Figure 2. Because of the difference, we do not make use of these element as inputs of the inverse rendering algorithm.

6 NOTATIONS TABLE

Table 1 provides the notations used in the main paper.

	Symbol	Description
Mueller Matrix and Stokes Vector	$\mathbf{M}$	General Mueller matrix
	$\mathbf{P}$	pBRDF
	$\mathbf{P}^{\mathrm{d,s}}$	Diffuse/specular pBRDF
	$\mathbf{H}$	Polarimetric shading
	$\mathbf{H}^{\mathrm{d,s}}$	Diffuse/specular polarimetric shading
	$\mathbf{C}_{\mathrm{i}\to\mathrm{n}}$	Coordinate conversion Muller matrix from light to plane of incidence
	$\mathbf{C}_{\mathrm{n}\to\mathrm{o}}$	Coordinate conversion from plane of incidence to camera system
	$\mathbf{F}^{\mathrm{T}}_{\mathrm{i,o}}$	Incident/exitant Fresnel transmission matrix.
	$\mathbf{F}^{\mathrm{R}}$	Fresnel reflection matrix.
	$\mathbf{D}$	depolarization matrix
	$\mathbf{L}$	Linear polarizer
	$\boldsymbol{\ell}$	First column of $\mathbf{L}$
	$\mathbf{\Phi}_{\mathrm{i,o}}$	Stacked matrix of $\boldsymbol{\ell}$ for incident/exitant polarizers
	$\mathbf{s}$	General Stokes vector consisting of four elements: $[s_0, s_1, s_2, s_3]$
	$\mathbf{s}_{\mathrm{before}}$	Stokes vector before an event
	$\mathbf{s}_{\mathrm{after}}$	Stokes vector after an event
	$\mathbf{s}_{\mathrm{i,o}}$	Stokes vectors of the light incident/exitant to an object surface.
Geometry	$\mathbf{y}_{\mathrm{i,o}}$	y-axis of the illumination/camera coordinate system.
	$\mathbf{n}$, $\mathbf{N}$	Normals of a pixel and its Matrix form for every pixel
	$\mathbf{n}_{\mathrm{b}}$, $\mathbf{N}_{\mathrm{b}}$	Normals from structured light and its Matrix form for every pixel
	$\mathbf{i}$	Illumination vector
	$\mathbf{o}$, $\mathbf{O}$	View vector and its Matrix form for every pixel
	$\mathbf{h}$, $\mathbf{\Psi}$	Half way vector and its matrix form for every pixel
	$\mathbf{h}_{\mathrm{i,o}}$	Projections of $\mathbf{h}$ to the incident/exitant polarization plane
	$\theta_{i,o}$	Zenith angle between normals and the incident/exitant light
	θ_h	Zenith angle between normals and halfway vector
	θ_d	Zenith angle between incident light and halfway vector
	$\phi_{i,o}$	Azimuth angle between the object plane of incidence and the y-axis of the incident/exitant
	$\varphi_{i,o}$	Azimuth angle between the micro-facet plane of incidence and the y-axis of the incident/exitant light
	$\vartheta_{i,o}$	Angle of the incident/exitant polarizers
	$\alpha_{i,o}$	$\alpha_{i,o} = \sin(2\phi_{i,o})$
	$\beta_{i,o}$	$\beta_{i,o} = \cos(2\phi_{i,o})$
	$\chi_{i,o}$	$\chi_{i,o} = \sin(2\varphi_{i,o})$
	$\gamma_{i,o}$	$\chi_{i,o} = \cos(2\varphi_{i,o})$
Reflectance	ρ	Diffuse albedo
	k_s	Specular coefficient
	σ	Surface roughness
	η	Refractive index
	G	Smith's shadowing/masking function
	D	GGX micro-facet distribution function
	C	Polarization-independent term of specular component
Polarization-related variables	ψ	Degree of polarization
	$\psi^{\mathrm{d}}_{\mathrm{i,o}}$	Diffuse degree of polarization of incident/exitant light
	δ	Phase shift
	$T_i^{\perp,\parallel}$	Fresnel incident transmission coefficients
	$T_o^{\perp,\parallel}$	Fresnel exitant transmission coefficients
	$T_{i,o}^+$	$(T_{i,o}^{\perp} + T_{i,o}^{\parallel})/2$
	$T_{i,o}^-$	$(T_{i,o}^{\perp} - T_{i,o}^{\parallel})/2$
	$R^{\perp,\parallel}$	Fresnel reflection coefficients
	R^+	$(R^{\perp} + R^{\parallel})/2$
	R^-	$(R^{\perp} - R^{\parallel})/2$
	$R^{\times}$	$\sqrt{R^{\perp}R^{\parallel}}$
Inverse Rendering	I	Pixel intensity
	n,m	Number of incidnet/extitant angles of polarizers
	B	Number of clusters
	w	Mask map of a cluster
	W	Confidence function penalizing pixels, of which normal is close to $\mathbf{h}$
	$\mathbf{W}$	Matrix form of W for every pixel
	W'	Confidence function weighting pixels with strong specular
	$\mathbf{W}'$	Matrix form of W' for every pixel
	$\mathbf{G}$	Gaussian blur matrix
	$\mathbf{C}_z$	Matrix-from of cosine values with the zenith angle
	$\mathbf{A}$	Collinearity matrix
	S	Half way angle-dependent function in $\mathbf{H}^{\mathrm{s}}_{00}$

Table 1. Symbols and notations used in the paper.

REFERENCES

Edward Collett. 2005. Field guide to polarization. SPIE Bellingham, WA.

Eric Heitz. 2014. Understanding the Masking-Shadowing Function in Microfacet-Based BRDFs. *J. Comput. Graph. Techn.* 3, 2 (2014), 48–107.

Achuta Kadambi, Vage Taamazyan, Boxin Shi, and Ramesh Raskar. 2015. Polarized 3D: High-Quality Depth Sensing with Polarization Cues. In *Proc. ICCV*. IEEE Computer Society, 3370–3378.

Bruce Walter, Stephen R Marschner, Hongsong Li, and Kenneth E Torrance. 2007. Microfacet models for refraction through rough surfaces. In *Eurographics conference on Rendering Techniques*. Eurographics Association, 195–206.